Terence E. Ryan,[1,2] Cameron A. Schmidt,[1,2] Thomas D. Green,[1,2]
Espen E. Spangenburg,[1,2] P. Darrell Neufer,[1,2] and Joseph M. McClung[1,2]

Targeted Expression of Catalase to Mitochondria Protects Against Ischemic Myopathy in High-Fat Diet–Fed Mice

Diabetes 2016;65:2553–2568 | DOI: 10.2337/db16-0387

Patients with type 2 diabetes respond poorly to treatments for peripheral arterial disease (PAD) and are more likely to present with the most severe manifestation of the disease, critical limb ischemia. The underlying mechanisms linking type 2 diabetes and the severity of PAD manifestation are not well understood. We sought to test whether diet-induced mitochondrial dysfunction and oxidative stress would increase the susceptibility of the peripheral limb to hindlimb ischemia (HLI). Six weeks of high-fat diet (HFD) in C57BL/6 mice was insufficient to alter skeletal muscle mitochondrial content and respiratory function or the size of ischemic lesion after HLI, despite reducing blood flow. However, 16 weeks of HFD similarly decreased ischemic limb blood flow, but also exacerbated limb tissue necrosis, increased the myopathic lesion size, reduced muscle regeneration, attenuated muscle function, and exacerbated ischemic mitochondrial dysfunction. Mechanistically, mitochondrial-targeted overexpression of catalase prevented the HFD-induced ischemic limb necrosis, myopathy, and mitochondrial dysfunction, despite no improvement in limb blood flow. These findings demonstrate that skeletal muscle mitochondria are a critical pathological link between type 2 diabetes and PAD. Furthermore, therapeutically targeting mitochondria and oxidant burden is an effective strategy to alleviate tissue loss and ischemic myopathy during PAD.

Type 2 diabetes is a major risk factor for peripheral arterial disease (PAD), and patients with type 2 diabetes typically present with PAD at earlier ages with accelerated disease evolution (1). In fact, diabetic patients with PAD are five times more likely to present clinically with critical limb ischemia (CLI) involving tissue loss (1) and typically do not respond efficiently to revascularization or endovascular interventions (2,3). The central and peripheral vascular mechanisms (2) of atherosclerotic disease exacerbation by type 2 diabetes are largely attributed to impaired arteriogenesis (4–8) and blunted angiogenesis (9,10). However, these vascular alterations fail to adequately address the effects on the functional deficits that accompany PAD, as type 2 diabetes also reduces limb muscle quality (11,12) and contributes to mitochondrial dysfunction (13). Although the initial insult in PAD is atherosclerotic occlusion, the reduced oxygen delivery to limb tissue induces an ischemic injury that manifests as a decline in muscle function (14–17). Limb skeletal muscle plays a critical role in determining morbidity and mortality in patients with PAD (18), and there is a strong association between muscle mitochondrial content and PAD mortality (19). These findings suggest that the affected limb muscle mitochondria may serve as an important site for the coalescence of type 2 diabetes and PAD pathology.

The development of type 2 diabetes has been intimately linked to chronic overnutrition via increased mitochondrial derived-oxidative stress and altered cellular redox homeostasis (13,20–23). Despite a well-known link between mitochondrial oxidative stress and cardiac ischemia (24), the role of aberrant skeletal muscle mitochondrial function in the increased susceptibility to ischemic myopathies in diabetic patients with PAD is not known. We hypothesized that the limb muscle mitochondrial dysfunction and oxidative stress caused by diet-induced overnutrition (high-fat diet [HFD]) would increase susceptibility of the murine peripheral limb to ischemia (hindlimb ischemia [HLI]). In

[1]East Carolina Diabetes and Obesity Institute, East Carolina University, Greenville, NC
[2]Department of Physiology, Brody School of Medicine, East Carolina University, Greenville, NC

Corresponding author: Joseph M. McClung, mcclungj@ecu.edu.

Received 25 March 2016 and accepted 25 May 2016.

this report, we demonstrate, using mice that are genetically resistant to ischemic pathology, that chronic HFD exacerbates myopathy, reduces mitochondrial function, decreases ischemic muscle contractile performance, and impairs recovery from HLI. Mechanistically, mitochondrial-targeted overexpression of catalase (MCAT) prevents tissue necrosis, muscle myopathy, contractile function, and mitochondrial respiration after HFD. These findings indicate that limb tissue mitochondria are a critical pathological link between diet and the severity of PAD manifestation and provide preclinical verification of the effectiveness of therapies targeting limb muscle mitochondrial respiratory function during ischemia combined with overnutrition.

RESEARCH DESIGN AND METHODS

Animals

Experiments were conducted on C57BL/6J (n = 56) mice (The Jackson Laboratory). Transgenic MCAT mice were a kind gift from Dr. Peter Rabinovitch (University of Washington) and maintained by crossing heterozygous MCAT males with female C57BL/6NJ mice (The Jackson Laboratory). All experiments involving MCAT mice (n = 28) were compared with wild-type (WT) littermates (n = 28) from the same breeders. Acute HLI (25,26) was induced by ligation and resection of the femoral artery inferior to the inguinal ligament and immediately proximal to the superficial caudal epigastric artery. The inferior epigastric, lateral circumflex, and superficial epigastric artery branches were left intact. A subcutaneous injection of buprenorphine (0.05 mg/kg) was administered postsurgery. The extent of necrosis in ischemic limbs was recorded postoperatively, by a blinded investigator when possible, using a semiquantitative scale (25,26). All work was approved by the Institutional Review Committee at East Carolina University. Animal care complied with the Guide for the Care and Use of Laboratory Animals, Institute of Laboratory Animal Resources, Commission on Life Sciences, National Research Council (Washington: National Academy Press, 1996). Mice were placed on either a 45% Kcal HFD (Research Diets D12451) or a 10% kcal low-fat diet (LFD; Research Diets D12450) at 6 weeks of age and maintained on the diet until sacrifice.

Reagents

All reagents were obtained from Sigma-Aldrich unless otherwise specified. The following commercial antibodies were used: CD31 (MCA-1364; AbD Serotec), smooth muscle actin (1A4; DakoCytomation), dystrophin (RB-9024; Thermo Scientific), total oxphos (110413; Abcam), GAPDH (MA5-15738; Thermo Scientific), and catalase (AB1877; Abcam). DAPI mounting medium (H-1200; Vector Laboratories) was used to coverslip slides. Secondary antibodies for immunofluorescence (IF) imaging were Alexa Fluor 488, 568, and 647 (A11006, A21134, and A21245, respectively; Invitrogen). Histological stains included Harris hematoxylin (26041-05; Sigma-Aldrich) and eosin (HT110132-1L; Sigma-Aldrich). Amplex Ultra Red was obtained from Invitrogen.

Assessment of Limb Perfusion and Tissue Oxygen Saturation

Limb blood flow was measured using laser Doppler perfusion imaging (LDPI) (26). Tissue oxygen saturation was assessed using a MoorVMS-OXY white light spectrometer with a CPT-300 optical probe (Moor Instruments).

Body Composition

Fat and lean body mass were determined using an EchoMRI-500 according to the manufacturer's instructions (EchoMRI).

Glucose and Insulin Tolerance Testing

Whole-body glucose tolerance was determined from intraperitoneal (IP) injection of glucose (2 g of glucose/kg lean body mass) after a 4-h fast (beginning in the last 3 h of the dark cycle). Insulin tolerance testing was performed using IP injections of insulin (0.75 U insulin/kg lean body mass) after a 4-h fast (beginning in the last 3 h of dark cycle).

IF and Histology

Skeletal muscle morphology and vessel density were assessed by standard light and IF microscopy. Standard methods for hematoxylin and eosin (H&E) were performed. Muscle regeneration and ischemic lesion area was performed on ×40 tiled H&E images using an Aperio CS2 digital slide analyzer (Leica Biosystems). Vascular density was performed by IF as previously described (26,27) and is presented as the mean percent $CD31^+$ (endothelial cell marker) or smooth muscle actin (SMA^+) area per ×20 field of view. All images were coded and randomized in order to allow for blinded analyses.

Immunoblotting

Western blotting was performed using standard methods.

Preparation of Isolated Skeletal Muscle Mitochondria for Respirometry

Skeletal muscle mitochondria were isolated from plantarflexor muscles of both control and ischemic limbs as previously described (28). High-resolution respirometry measurements were conducted using the OROBOROS O2K Oxygraph (Oroboros Instruments) as previously described (28). The rate of respiration was expressed as picomoles per second per milligram mitochondrial protein.

Mitochondrial H_2O_2 Emission Measurement

Mitochondrial H_2O_2 emission was measured fluorometrically at 37°C via Amplex Ultra Red (10 μmol/L)/horseradish peroxidase (3 U/mL) detection system (excitation/emission 565/600) (28).

Citrate Synthase Activity

Citrate synthase activity assays were performed using a commercially available kit (CS0720; Sigma-Aldrich).

Muscle Contractile Force Measurements

Contractile force measurements were performed using extensor digitorum longus (EDL) muscles (29). Muscle output was expressed as specific force (N/cm^2) determined by dividing the tension (N) by the muscle cross-sectional area (30).

Measurements of Cellular Redox State

Reduced glutathione (GSH) and glutathione disulfide (oxidized [GSSG]) were measured in EDL muscle by high-performance liquid chromatography (31,32).

Statistics

Data are presented as mean ± SEM. Statistical analyses were performed using Prism 6 (v. 6.0d; GraphPad) software and Vassarstats (www.vassarstats.net). Comparisons between

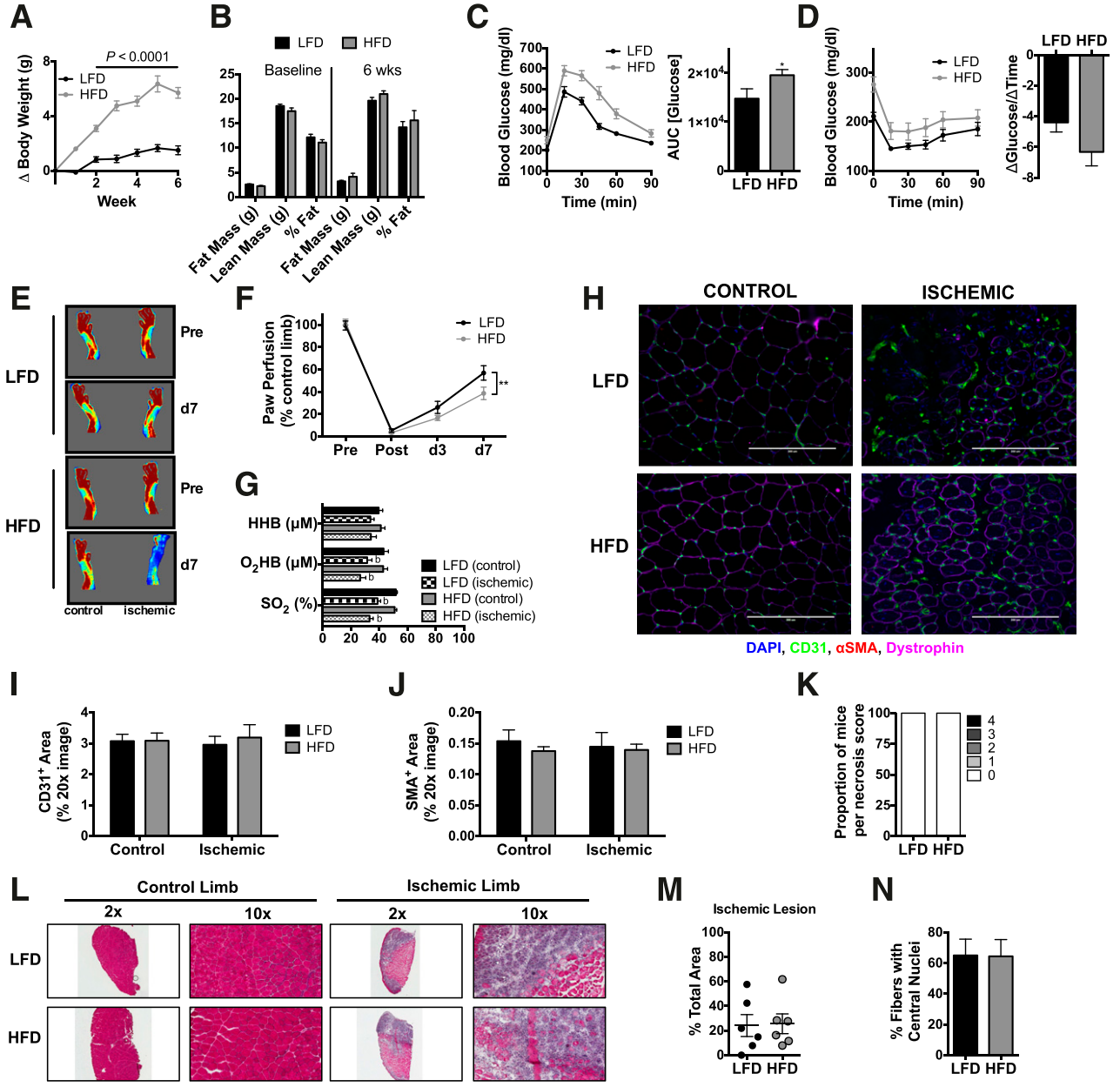

Figure 1—Short-term high-fat feeding does not exacerbate ischemic pathology. *A*: Body weight gain during 6 weeks of HFD and LFD. *B*: Body composition measurements using EchoMRI at baseline and 6 weeks for HFD (n = 12) and LFD (n = 12) mice. *C*: Compared with LFD mice (n = 12), HFD mice (n = 12) were glucose intolerant following an IP glucose tolerance test. *D*: Insulin tolerance of HFD (n = 12) and LFD (n = 12) mice. *E*: Representative LDPI images pre-HLI and 7 days post-HLI (d7). *F*: Quantification of LDPI flux shows lower paw perfusion recovery in HFD mice (n = 12) compared with LFD mice (n = 12). *G*: Paw tissue oxygenation, oxygenated hemoglobin/myoglobin, and deoxygenated hemoglobin were not different between HFD (n = 8) and LFD (n = 8) mice 7 days post-HLI. *H*: Representative IF images of the TA muscle from control and ischemic limbs of HFD and LFD mice. *I*: $CD31^+$ area from LFD and HFD mice (n = 6/group). *J*: SMA^+ area from LFD and HFD mice (n = 6/group). *K*: Proportions of necrosis scores between HFD and LFD mice were not different (n = 12/group). *L*: Representative H&E stains of the control and ischemic limbs of HFD and LFD mice. *M*: Quantification of the ischemic lesion area (consisting of anucleate necrotic myofibers) was not different between HFD and LFD mice (n = 6/group). *N*: The percentage of fibers with centralized nuclei was not different between HFD and LFD mice (n = 6/group). Data are mean ± SEM and were compared with two-way ANOVA followed by Tukey posttest or two-tailed Student t test. Nonparametric data (necrosis scores) were compared with Mann-Whitney test. Scale bars: 200 μm. $^*P < 0.05$, $^{**}P < 0.01$, and $^bP < 0.05$ for ischemia effect. AUC, area under the curve; wks, weeks.

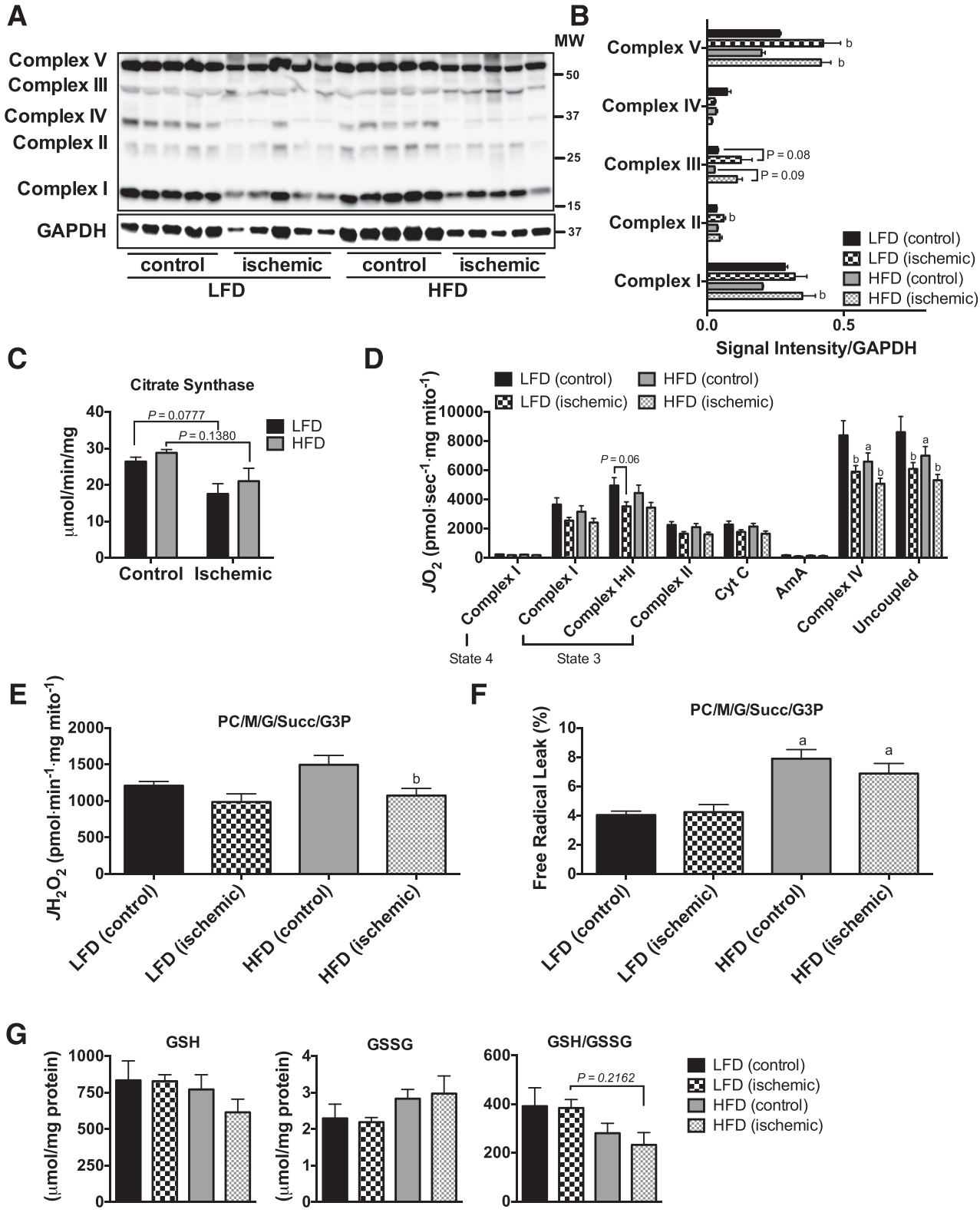

Figure 2—Short-term high-fat feeding does not alter mitochondrial content or respiratory function. *A*: Western blotting for mitochondrial ETS proteins on control and ischemic limb EDL muscle from HFD and LFD mice (n = 5/group). *B*: Densitometry of Western blotting shows no diet effects on the abundance of proteins in the ETS. *C*: Citrate synthase activity was also not different between diets and only marginally lower in ischemic limbs. *D*: High-resolution respirometry experiments performed on isolated skeletal muscle mitochondria show that the respiratory capacity was similar between HFD and LFD mice (n = 6/group). *E*: Mitochondrial H_2O_2 emission under state 4 conditions with 25 μmol palmitoyl carnitine, 10 mmol glutamate, 2 mmol malate, 10 mmol succinate, and 10 mmol glycerol-3-phosphate. *F*: Free radical leak (%), calculated by normalizing data from *E* by state 4 JO_2 measured in parallel experiments under identical substrate conditions, was greater in HFD mice (n = 6/group). *G*: GSH, GSSG (oxidized form), and the GSH/GSSG ratio were not statistically different

two groups were performed by Student two-tailed *t* test. Comparisons of data with more than two groups were performed using two-way ANOVA with Tukey post hoc multiple comparisons. Repeated-measures ANOVA were conducted when appropriate. Nonparametric Mann-Whitney testing was used to determine differences between the distributions of necrosis scores between groups. In all cases, $P < 0.05$ was considered statistically significant.

RESULTS

Short-Term High-Fat Feeding Does Not Worsen Ischemic Limb Pathology

We initially fed C57BL/6J mice, a parental strain of mice characterized to be resistant to ischemic myopathy (25,27), a 45% HFD or 10% LFD for 6 weeks. This duration of HFD was chosen on the basis of the knowledge that whereas mitochondrial oxidant emitting potential may be increased (20), mitochondrial respiratory function and content remain unchanged (21). Mice on the HFD gained more weight and body fat (Fig. 1*A* and *B*) and developed whole-body glucose intolerance (Fig. 1*C*). After 7-day HLI, mice on HFD had reduced blood flow in the paw (Fig. 1*E* and *F*), although no differences in paw tissue oxygenation were detected (Fig. 1*G*). IF microscopy revealed no differences in $CD31^+$ (Fig. 1*H* and *I*) or SMA^+ (Fig. 1*J*) density in the ischemic limbs. Additionally, there was no diet-induced ischemic tissue loss/necrosis (Fig. 1*K*). The ischemic lesion area, identified by H&E staining for anucleate necrotic fibers, was not altered by acute HFD prior to HLI (Fig. 1*L* and *M*). Moreover, the percentage of fibers with centralized nuclei, a hallmark of muscle regeneration, was also not altered by diet (Fig. 1*N*).

Short-Term High-Fat Feeding Increases Mitochondrial H_2O_2 Emission but Does Not Alter Respiratory Function

Similar to previous work (21), we found no evidence of overt decreases in mitochondrial content, measured by Western blotting for the complexes in the electron transport system (ETS) (Fig. 2*A* and *B*). Citrate synthase activity trended lower in the ischemic limbs of both groups (Fig. 2*C*). Mitochondrial respiratory function was not altered by HFD in either control or ischemic limbs across most substrate conditions (Fig. 2*D*), although detectable differences in ischemic Complex IV and uncoupled respiration were detected for both diet conditions after HLI. Six weeks of HFD did not significantly alter mitochondrial H_2O_2-emitting potential (Fig. 2*E*), but increased the calculated percent free radical leak (JH_2O_2 normalized by JO_2) in HFD mice (Fig. 2*F*). Cellular redox state was analyzed by measuring GSH and GSSG levels in the EDL muscle (Fig. 2*G*). The ratio of GSH/GSSG did not reach statistical significance (all $P > 0.2$) in either control or ischemic limbs of HFD mice.

Chronic High-Fat Feeding Exacerbates Ischemic Limb Pathology

Because we found no apparent effects of short-term HFD on ischemic necrosis or myopathy, we next performed identical experiments on mice consuming an HFD for 16 weeks, a duration known to induce oxidative stress and mitochondrial dysfunction (21). As expected, 16-week HFD resulted in greater weight gain (Fig. 3*A*), substantial increases in fat mass (Fig. 3*B*), whole-body glucose intolerance (Fig. 3*C*), and reduced insulin sensitivity (Fig. 3*D*). Following HLI, paw blood flow was again impaired in HFD mice (Fig. 3*E* and *F*), but no diet-induced alterations in paw tissue oxygenation were found (Fig. 3*G*). IF microscopy revealed no differences in $CD31^+$ or SMA^+ density in the ischemic limbs (Fig. 3*H*–*J*). Strikingly, 16-week HFD resulted in significantly greater limb necrosis (Fig. 3*K*) after HLI, a greater tibialis anterior (TA) ischemic lesion area (Fig. 3*L* and *M*), and reduced muscle regeneration (Fig. 3*N*). These findings are of particular interest given that C57BL/6 mice are known to recover rapidly from limb ischemia without tissue necrosis (25,27). To determine whether the exacerbated ischemic myopathy had functional implications, we performed force-frequency contractile measurements in isolated EDL muscles. Chronic HFD did not decrease force production in the control limb. A substantial loss of force was observed, however, in the HFD ischemic limb (Fig. 3*O* and *P*). Collectively, these findings indicated the presence of a substantial HFD-induced ischemic myopathy after 16 weeks of overnutrition.

Chronic High-Fat Feeding Increases Mitochondrial H_2O_2-Emitting Potential and Reduces Respiratory Function

Immunoblotting for the protein complexes of the ETS revealed no major alterations in the abundance of ETS proteins with diet or ischemia (Fig. 4*A* and *B*). Citrate synthase activity was not altered by 16-week HFD, but was significantly reduced after ischemia in both HFD and LFD mice (Fig. 4*C*). Sixteen weeks of HFD decreased the mitochondrial respiratory capacity under multiple substrate conditions (Fig. 4*D*). HLI resulted in marginal

between diets, although muscle from HFD tended to exhibit lower GSH/GSSG (n = 5/group). Data are mean ± SEM and were compared with two-way ANOVA followed by Tukey posttest or two-tailed Student *t* test. [a]$P < 0.05$ for diet effect, [b]$P < 0.05$ for ischemia effect. AmA, antimycin A; Complex $I_{(state\ 3)}$, glutamate + malate + adenosine diphosphate; Complex $I_{(state\ 4)}$, glutamate + malate; Complex $I+II_{(state\ 3)}$, glutamate + malate + adenosine diphosphate + succinate; Complex $II_{(state\ 3)}$, glutamate + malate + adenosine diphosphate + succinate + rotenone; Complex IV, ascorbate + N,N,N',N'-tetramethyl-p-phenylenediamine; Cyt C, cytochrome c; G, glutamate; G3P, glycerol-3-phosphate; M, malate; MW, molecular weight; PC, palmitoyl carnitine; Succ, succinate; Uncoupled, carbonyl cyanide-4-(trifluoromethoxy)phenylhydrazone.

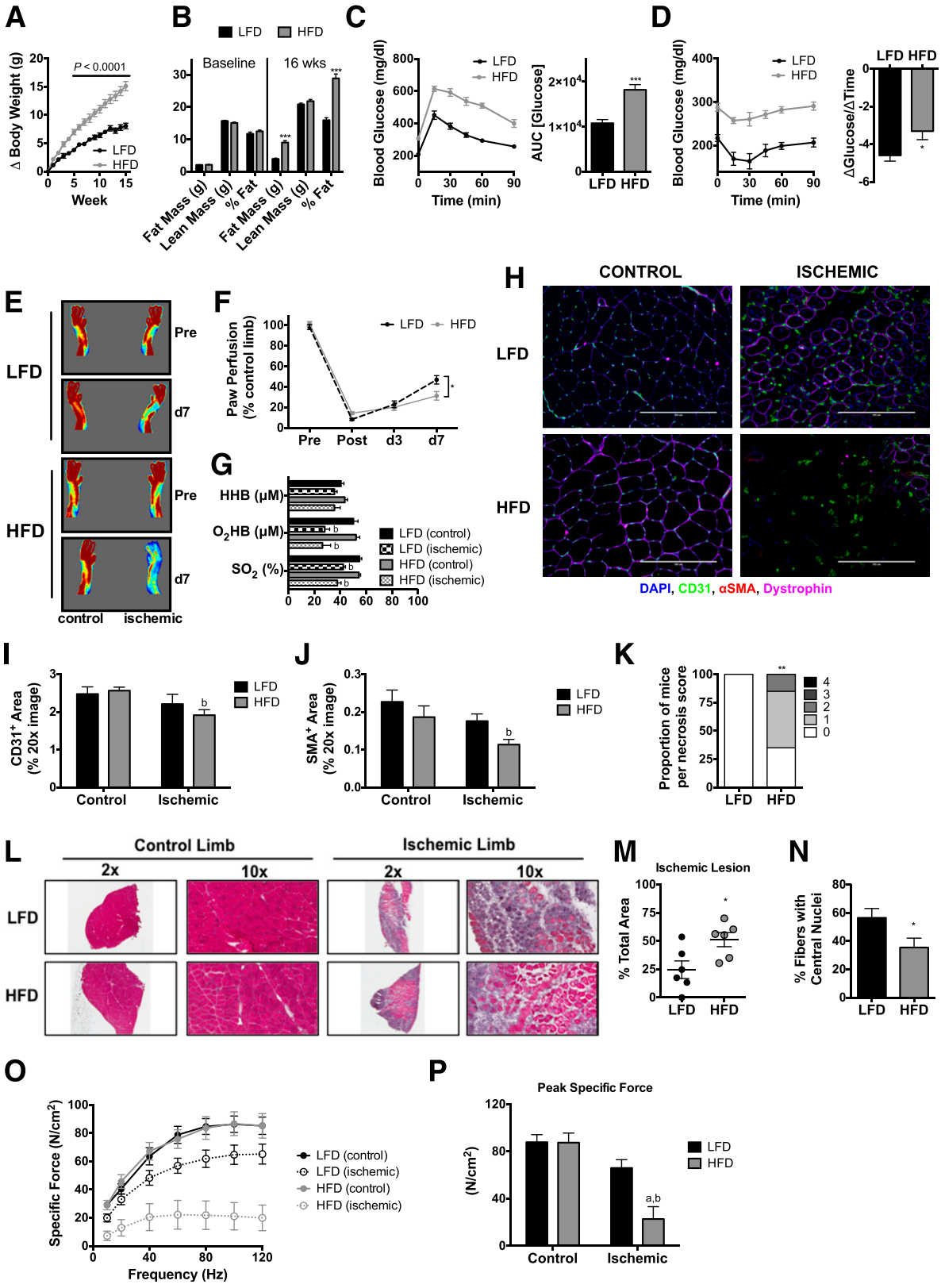

Figure 3—Chronic high-fat feeding exacerbates ischemic pathology and reduces muscle contractile performance. *A*: Body weight gain during 16 weeks of HFD and LFD. *B*: Body composition measurements using EchoMRI at baseline and 16 weeks for HFD (n = 16) and LFD (n = 16) mice. *C*: Compared with LFD mice (n = 16), HFD mice (n = 16) were glucose intolerant following an IP glucose tolerance test. *D*: Insulin tolerance of HFD (n = 16) and LFD (n = 16) mice. *E*: Representative LDPI images pre-HLI and 7 days post-HLI (d7). *F*: Quantification of LDPI flux shows lower paw perfusion recovery in HFD mice (n = 16) compared with LFD mice (n = 16). *G*: Paw tissue oxygenation, oxygenated hemoglobin/myoglobin, and deoxygenated hemoglobin were not different between HFD (n = 13) and LFD (n = 14) mice 7 days post-HLI. *H*: Representative IF images of the TA muscle from control and ischemic limbs of HFD and LFD mice. *I*: $CD31^+$ area from LFD and HFD mice (n = 6/group). *J*: SMA^+ area from LFD and HFD

decreases in respiratory capacity in LFD mice only under ADP-stimulated complex I–supported, complex IV–supported, and uncoupled respiration. Strikingly, HLI resulted in an even further decrease in respiratory capacity in HFD mice (Fig. 4*D*), suggesting that mitochondriopathy occurs as part of limb pathology in a murine model of diabetic PAD. Similar to the short-term HFD, chronic HFD elevated mitochondrial H_2O_2-emitting potential in skeletal muscle mitochondria isolated from the control limb (Fig. 4*E* and *F*). Interestingly, ischemia did not increase mitochondrial H_2O_2 emission or the percent free radical leak in either LFD or HFD mice. In fact, H_2O_2 emission was reduced in HFD ischemic limb mitochondria. Analysis of the cellular redox state indicated reduced GSH, increased GSSG, and a marked reduction in the GSH/GSSG ratio after HFD (Fig. 4*G*) that was not exacerbated by HLI.

Mitochondrial-Targeted Overexpression of Catalase Prevents HFD-Induced Ischemic Myopathy

Chronic overnutrition results in an oversupply of reducing equivalents (NADH and flavin adenine dinucleotide) to complex I and the quinone pool of the electron transport system, elevating the mitochondrial membrane potential and increasing the likelihood of reactive oxygen species (ROS) such as superoxide and hydrogen peroxide (13). As a result, chronic oxidative stress impairs mitochondrial respiratory function and structure and reduces mitochondrial density and gene expression related to mitochondrial biogenesis (21). Therefore, we reasoned that increased redox buffering during chronic overfeeding, which would decrease the chronic oxidative stress and could maintain mitochondrial respiratory function, might prevent the ischemic myopathy associated with chronic HFD. We used a transgenic mouse developed to overexpress human catalase (which breaks down H_2O_2) targeted to the mitochondria (33,34). Because the catalase transgene in these mice is driven by a β-actin promoter, we first characterized the expression of catalase in various tissues of WT and MCAT mice. Western blotting revealed that catalase overexpression was robust in heart and skeletal muscle, but not in the kidney or liver (also mitochondrial dense tissues) (Fig. 5), which is consistent with findings from the original founder lines of these mice (33). Importantly, we only detected a marginal increase in catalase expression in femoral arteries isolated from these mice (Fig. 5).

MCAT mice and their WT littermates were placed on an HFD for 16 weeks. MCAT mice gained the same amount of body weight and body fat as WT littermates (Fig. 6*A* and *B*) and exhibited similar glucose intolerance and insulin sensitivity (Fig. 6*C* and *D*). Ischemic paw blood flow (Fig. 6*E* and *F*) and tissue oxygenation (Fig. 6*G*) were unchanged by MCAT overexpression (compared with WT). IF staining for endothelial cell ($CD31^+$ area) and SMA^+ area markers was also unaltered by MCAT overexpression following HFD and ischemia (Fig. 6*H–J*). MCAT overexpression reduced necrotic tissue loss (Fig. 6*K*), ischemic lesion size (Fig. 6*L* and *M*), and increased muscle regeneration (Fig. 6*N*) after HLI. Remarkably, MCAT overexpression also rescued the 16-week HFD-induced deficit in contractile function of the ischemic limb muscle (Fig. 6*O* and *P*).

Mitochondrial-Targeted Overexpression of Catalase Prevents HFD-Induced Mitochondrial Function in Ischemic Limb Muscle

Muscle mitochondrial content, assessed by Western blotting (Fig. 7*A* and *B*) and citrate synthase activity (Fig. 7*C*), indicated that there were no effects of MCAT overexpression on mitochondrial content during HFD and/or HLI. High-resolution respirometry revealed that MCAT overexpression prevents impairments in ischemic mitochondrial respiration under multiple substrate conditions after 16-week HFD (Fig. 7*D*). Consistent with previous work (20), mitochondrial H_2O_2 emission was much lower in MCAT mice (Fig. 7*E* and *F*) at baseline and was unaffected by HLI. Assessment of the cellular redox state in EDL muscle indicated a more reduced environment (i.e., higher GSH/GSSG ratio), which is consistent with enhanced redox buffering networks (Fig. 7*G*).

Mitochondrial-Targeted Overexpression of Catalase Does Not Enhance Ischemic Recovery in Chow-Fed Mice

Previous studies have suggested that increased oxidative stress may play a role in tissue pathology in PAD (16,17,35,36). Lastly, we sought to determine whether mitochondrial catalase overexpression was sufficient, in the absence of HFD, to reduce the severity of HLI pathology. Following HLI, paw blood flow recovery (Fig. 8*A* and *B*) was identical between WT and MCAT mice. There was no observed tissue necrosis in either WT or MCAT ischemic limbs (Fig. 8*D*). Mitochondrial respiratory capacity (Fig. 8*C*) was also identical between WT and MCAT mice after HLI. As expected, mitochondrial H_2O_2 emission (Fig. 8*D*) and free radical leak (Fig. 8*E*) were lower in MCAT

mice (n = 6/group). *K*: Proportions of necrosis scores were greater in HFD mice compared with LFD mice (n = 16/group). *L*: Representative H&E stains of the control and ischemic limbs of HFD and LFD mice. *M*: Quantification of the ischemic lesion area (consisting of anucleate necrotic myofibers) was significantly larger in HFD mice compared with LFD mice (n = 6/group). *N*: The percentage of fibers with centralized nuclei was lower in HFD compared with LFD mice (n = 6/group). *O*: Force-frequency relationships in isolated EDL muscles from control and ischemic limbs in HFD and LFD mice (n = 8/group). *P*: Peak specific force was significantly lower in the ischemic limb of HFD mice. Data are mean ± SEM and were compared with two-way ANOVA followed by Tukey posttest or two-tailed Student t test. Nonparametric data (necrosis scores) were compared with Mann-Whitney test. HHB, deoxygenated hemoglobin/myoglobin; O_2HB, oxygenated hemoglobin/myglobin; SO_2, tissue saturation. Scale bars: 200 μm. $^*P < 0.05$, $^{**}P < 0.01$, $^{***}P < 0.001$, $^aP < 0.05$ for diet effect, $^bP < 0.05$ for ischemia effect. AUC, area under the curve; wks, weeks.

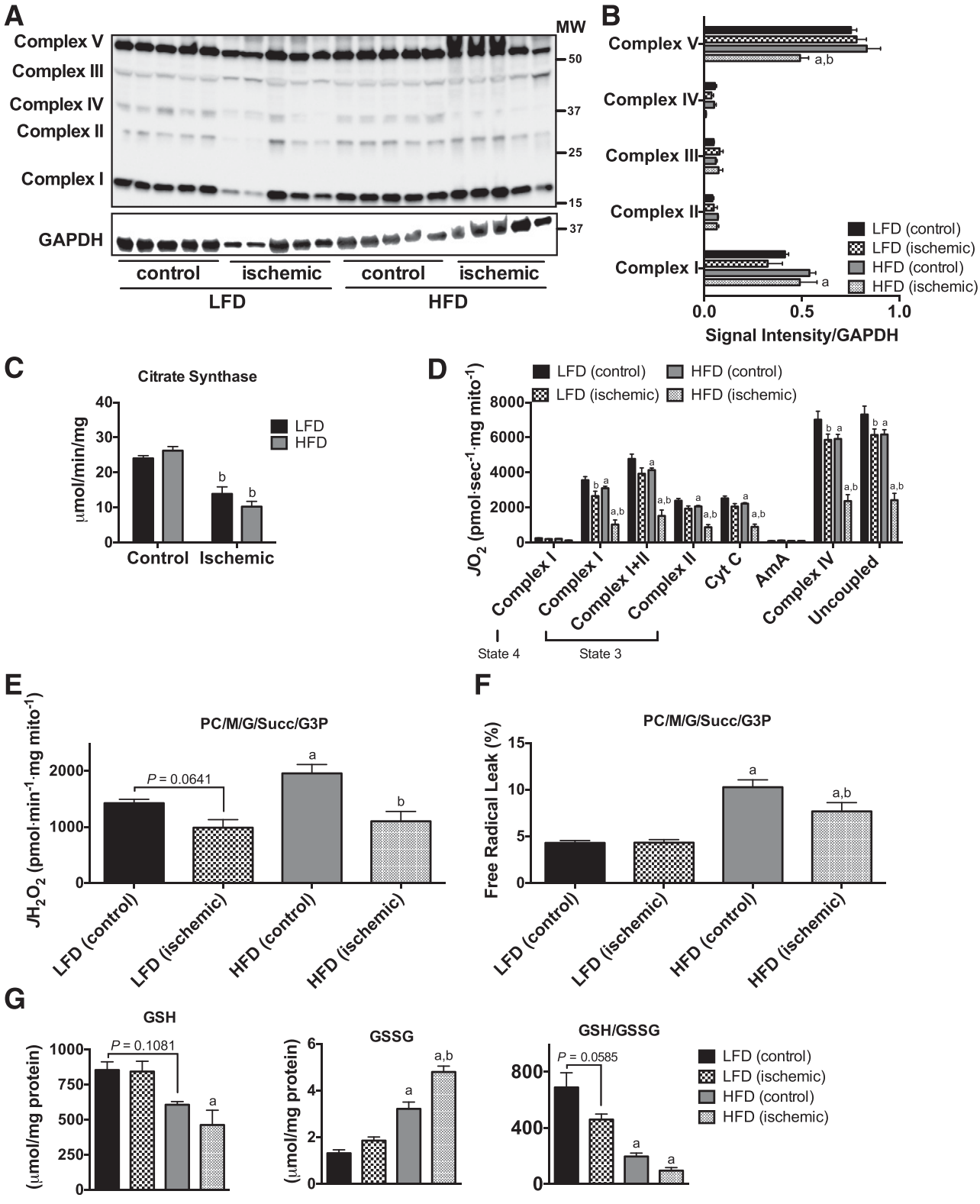

Figure 4—Chronic high-fat feeding does not alter mitochondrial content but reduces respiratory function and increases mitochondrial H_2O_2-emitting potential. *A*: Western blotting for mitochondrial ETS proteins on control and ischemic limb EDL muscle from HFD and LFD mice (n = 5/group). *B*: Densitometry of Western blotting shows no major diet effects on the abundance of proteins in the ETS except for Complex V, which was lower in HFD ischemic limb muscle. *C*: Citrate synthase activity was also not different between diets but was decreased in ischemic limbs of both HFD and LFD mice (n = 5/group). *D*: High-resolution respirometry experiments performed on isolated skeletal muscle mitochondria show that the respiratory capacity was lower in HFD control limbs compared with those of LFD (n = 8/group), which was further reduced following HLI. *E*: Mitochondrial H_2O_2 emission under state 4 conditions with 25 μmol palmitoyl carnitine, 10 mmol glutamate, 2 mmol malate, 10 mmol succinate, and 10 mmol glycerol-3-phosphate was elevated in the control limbs of HFD mice but did not increase further following HLI (n = 8/group). *F*: Free radical leak (%), calculated by normalizing data from *E* by state 4 JO_2

mice. Collectively, these data demonstrated that, in the absence of a preexisting mitochondria stressor (such as chronic HFD), targeted catalase overexpression is not an effective therapy for further improving ischemic pathology in mice from the C57BL/6NJ background.

DISCUSSION

The mechanisms behind why patients with PAD with type 2 diabetes experience more severe pathology and respond worse to endovascular or revascularization surgical interventions (37) are unclear. To the best of our knowledge, this is the first report to investigate the efficacy of therapeutically targeting mitochondria in a preclinical PAD model with diet-induced type 2 diabetes. Our findings revealed that: *1*) short-term HFD (6 weeks) does not exacerbate ischemic necrosis, myopathy, or mitochondriopathy during limb ischemia despite reducing limb blood flow; *2*) chronic HFD (16 weeks) increases ischemic necrosis, myopathy, mitochondriopathy, and H_2O_2 emission in conjunction with reduced limb blood flow; *3*) mitochondrial targeted overexpression of catalase is sufficient to rescue chronic HFD-induced exacerbations of ischemic necrosis, myopathy, mitochondriopathy, and H_2O_2 emission; and *4*) a preexisting stressor (in this case, HFD) is required for MCAT to demonstrate efficacy as a therapeutic adjuvant during ischemia.

Skeletal muscle from obese patients and patients with type 2 diabetes is characterized by depressed electron transport system activity, reduced expression of genes related to oxidative metabolism, altered mitochondrial morphology, and lower mitochondrial content (38–40). Further, the development of muscle insulin resistance has been intimately linked to mitochondrial-derived oxidants (i.e., H_2O_2) (13,20,22,23). Chronic overnutrition, which is closely associated with type 2 diabetes, results in an oversupply of reducing equivalents (i.e., NADH and flavin adenine dinucleotide from upstream catabolism) to the mitochondrial electron transport system. The consequence is an elevation in the mitochondrial membrane potential, which, in the absence of increased metabolic demand, increases the pressure in the ETS and the likelihood that electrons can leak from the system to form ROS (i.e., superoxide anion). In the context of chronic HFD, Bonnard et al. (21) demonstrated that long-term HFD increases oxidative stress in skeletal muscle and results in altered mitochondrial morphology, decreased mitochondrial content, and attenuated respiratory function. Considering that mitochondria serve as a principle source of ATP, oxidants (41,42), and reducing equivalents required for redox buffering (i.e., NADPH) (28), mitochondria appear to be an attractive candidate for therapeutic intervention in situations in which multiple risk factors coalesce to magnify the consequences of reduced ATP availability and increased oxidative stress, such as occurs in the degenerative/regenerative microenvironment of the ischemic limb.

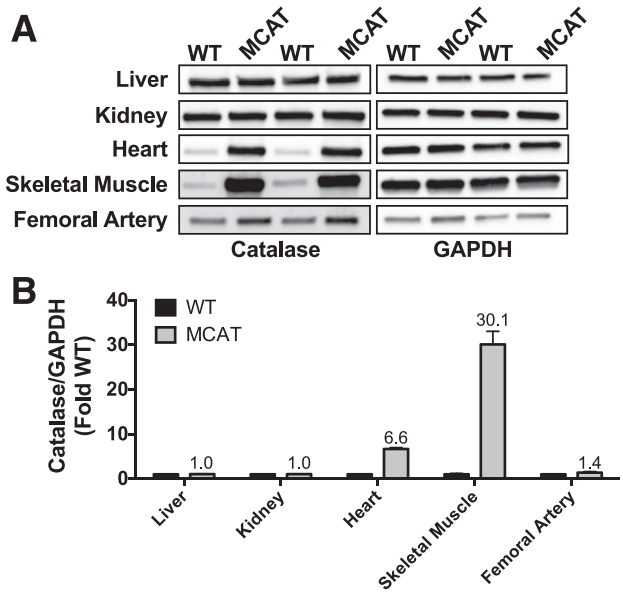

Figure 5—Catalase overexpression occurs primarily in heart and skeletal muscle. *A*: Representative Western blots for catalase demonstrate that robust overexpression occurs primarily in heart and skeletal muscle, but not liver, kidney, or the femoral artery in MCAT mice compared with WT littermates (n = 3/tissue). GAPDH was used as a loading control, and confirmation of even loading was performed from quantification of total protein loaded in the polyvinylidene difluoride membrane. *B*: Quantification of Western blots for catalase/GAPDH, expressed as fold change from the WT for each tissue.

Previous work using shorter durations of high-fat feeding (6–12 weeks) has linked mitochondrial H_2O_2 production/emission and a more oxidized cellular redox environment to the development of insulin resistance in skeletal muscle (20). In those studies, MCAT mice on an

measured in parallel experiments under identical substrate conditions, was greater in the control and ischemic limbs of HFD mice compared with those of LFD mice, but was significantly decreased in the ischemic limbs compared with control limb mitochondria (n = 8/group). *G*: GSH was significantly lower in the ischemic limbs of HFD mice compared with LFD ischemic limbs; GSSG, oxidized form, was elevated in both control and ischemic limbs of HFD mice compared with those of LFD mice, and a further increase in GSSG was evident in HFD, but not LFD, ischemic muscle; and the GSH/GSSG ratio was substantially lower in HFD control and ischemic muscle compared with LFD muscle, but no effect of ischemia was detected in either group (n = 5/group). Data are mean ± SEM and were compared with two-way ANOVA followed by Tukey posttest or two-tailed Student t test. $^aP < 0.05$ for diet effect, $^bP < 0.05$ for ischemia effect. AmA, antimycin A; Complex $I_{(state\ 3)}$, glutamate + malate + adenosine diphosphate; Complex $I_{(state\ 4)}$, glutamate + malate; Complex $I+II_{(state\ 3)}$, glutamate + malate + adenosine diphosphate + succinate; Complex $II_{(state\ 3)}$, glutamate + malate + adenosine diphosphate + succinate + rotenone; Complex IV, ascorbate + N,N,N',N'-tetramethyl-p-phenylenediamine; Cyt c, cytochrome c; G, glutamate; G3P, glycerol-3-phosphate; M, malate; MW, molecular weight; PC, palmitoyl carnitine; Succ, succinate; Uncoupled, carbonyl cyanide-4-(trifluoromethoxy)phenylhydrazone.

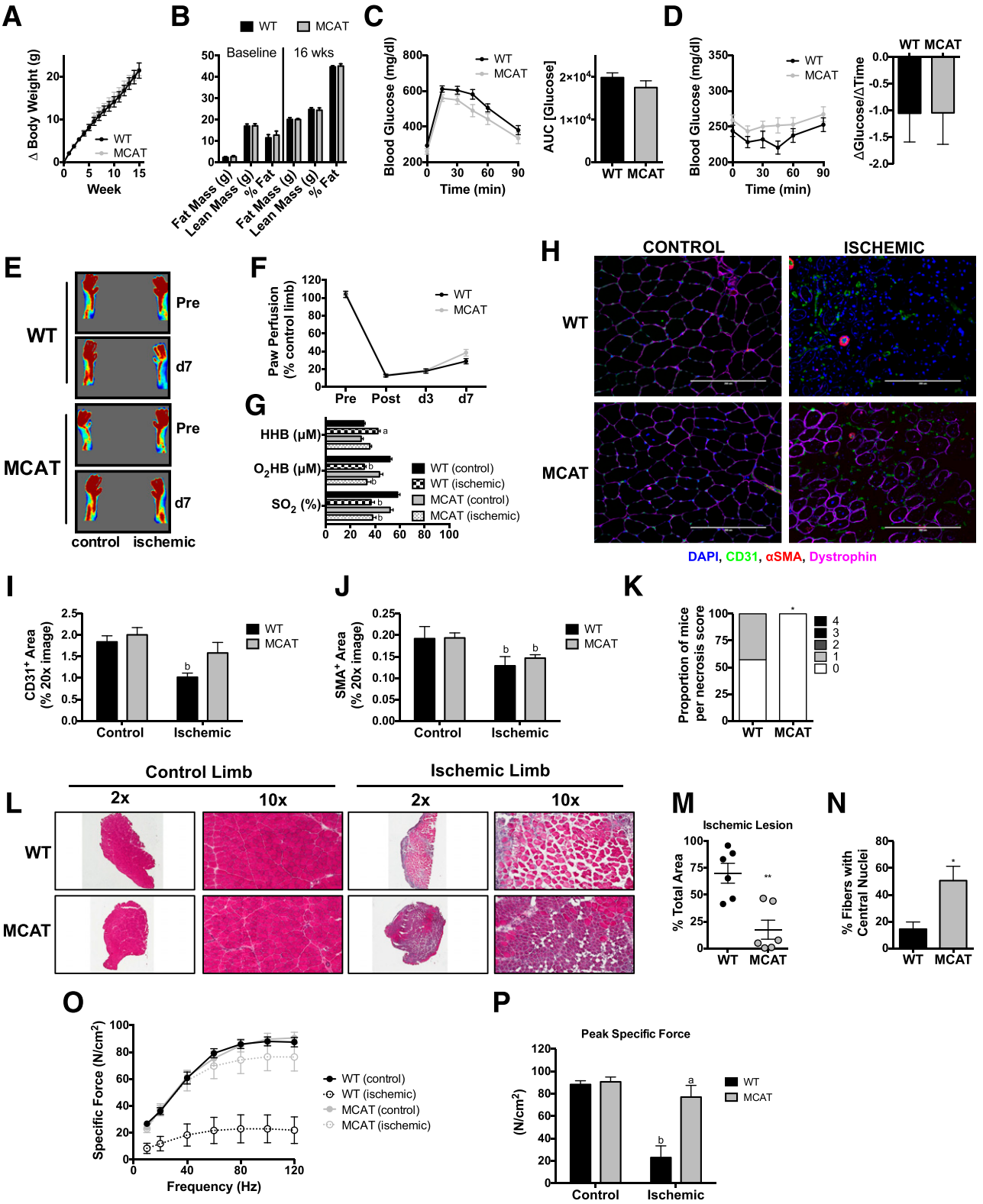

Figure 6—MCAT rescues ischemic pathology and muscle contractile performance in chronic HFD-fed mice. *A*: Body weight gain during 16 weeks was not different between WT and MCAT. *B*: Body composition measurements using EchoMRI at baseline and 16 weeks for WT (n = 12) and MCAT (n = 12) mice. *C*: WT mice (n = 8) and MCAT mice (n = 8) were both glucose intolerant following an IP glucose tolerance test. *D*: Insulin tolerance of WT (n = 8) and MCAT (n = 8) mice. *E*: Representative LDPI images pre-HLI and 7 days post-HLI (d7). *F*: Quantification of LDPI flux demonstrates that paw perfusion recovery was not different between WT mice (n = 24) and MCAT mice (n = 24). *G*: Paw tissue oxygenation, oxygenated hemoglobin/myoglobin, and deoxygenated hemoglobin were not different between WT (n = 6) and MCAT (n = 6) mice 7 days post-HLI. *H*: Representative IF images of the TA muscle from control and ischemic limbs of WT and MCAT mice. *I*: $CD31^+$ area from WT and MCAT mice (n = 6/group). *J*: SMA^+ area from WT and MCAT mice (n = 6 mice/group). *K*: Proportions of necrosis scores were greater in WT mice

HFD did not display elevated mitochondrial H_2O_2 emission and were protected from developing insulin resistance at the whole-body and skeletal muscle levels (assessed by hyperinsulinemic-euglycemic clamp). In the current study, mice were maintained on an HFD longer (>16 weeks), which resulted in all groups displaying some degree of glucose intolerance, including the MCAT mice. High-fat feeding beyond 12 weeks in mice is associated with progressive deterioration in metabolic function in several tissues, including skeletal muscle and liver (21,43–45). The persistent oxidant burden from the HFD is thought to gradually overwhelm antioxidant defense systems, leading to organelle damage and eventual failure. MCAT mice have increased antioxidant capacity primarily in skeletal and cardiac muscle only, and thus, it is not likely that MCAT mice will be completely protected from a chronic high-fat feeding, particularly at the whole-body level where other tissues (i.e., liver and pancreas) contribute to the response following administration of a glucose bolus. This undoubtedly reflects the complex relationship between cellular redox homeostasis and insulin resistance/diabetes.

Mitochondrial-derived ROS have been strongly linked to cardiac ischemia-reperfusion injury (24), and increased markers of oxidative stress (i.e., 4-hydroxynonenal, protein carbonyls, and lipid peroxides) are present in both clinical PAD tissue samples and limb muscle from rodent preclinical models (35,36). In our experiments, 7 days of HLI did not dramatically shift cellular redox toward an oxidative state. In fact, our quantitative measurements of mitochondrial H_2O_2 emission were consistently lower in the ischemic limb and accompanied by a largely unaffected free radical leak (calculated by normalizing JH_2O_2 to JO_2 under identical experimental conditions). Discrepancies between the current study and previous work (35,36) are likely due to experimental approaches, as these previous studies only measured indirect markers of oxidative stress, whereas direct measurements of mitochondrial H_2O_2 emission were made in this study. In the current study, we used a fluorescent probe (Amplex UltraRed; Invitrogen), which is highly specific for H_2O_2 and provides sensitive and accurate measurements under experimental conditions designed to specifically identify mitochondrial-derived H_2O_2. In contrast, measurement of 4-hydroxynonenal, protein, lipid, and DNA oxidation only provide global evidence of damage that cannot be linked to specific reactive oxygen or nitrogen species and is often prone to artifacts during sample preparation. Our findings seem logical based on bioenergetic requirements of both electron flow and oxygen content, which are limited during hypoxia. This is consistent with findings in cardiac mitochondria, in which electron-carrying reducing equivalents and upstream metabolites build up during ischemia, and ROS production increases upon reperfusion when oxygen levels return (24).

In addition to mitochondrial dysfunction, type 2 diabetes is also associated with reduced muscle quality (11,12) and sarcopenic obesity. Clinically, reduced muscle function is especially concerning for patients with PAD, considering that muscle strength/performance and exercise tolerance are the strongest predictors of mortality (14,18,46–49). These results suggest that preexisting impairments in mitochondrial and muscle function may worsen ischemic limb pathology once atherosclerotic lesions substantially begin to affect limb blood flow. The observed mitochondrial stress derived from a 16-week HFD was associated with a worsening of ischemic injury and blunted muscle regeneration following HLI. These findings are consistent with previous reports demonstrating that chronic HFD impairs muscle regeneration in nonischemic models of muscle injury (50,51). The consequences of chronic HFD superimposed on limb ischemia are impressive when examined in the context of the limb muscle's contractile function. Our analysis revealed a 75% reduction in peak specific force after ischemia (compared with a ~25% reduction in LFD mice). This corresponded with greater tissue loss/necrosis and substantial reductions in indicators of muscle regeneration. Importantly, all experiments performed in this study involved mice on the C57BL/6 genetic background, which is a parental strain largely resistant to ischemic myopathy that rarely displays appreciable tissue loss/necrosis (25,26). This makes the appearance of ischemic paw necrosis and muscle myopathies in the HFD-fed mice even more astonishing and implies that environmental factors, such as chronic overnutrition, can override inherent genetic protection from ischemia.

It is reasonable to assume that the ischemic myopathy observed in our study could be attributed, at least in part, to impaired angiogenesis/arteriogenesis or collateral rarefaction as a result of chronic HFD. Previous reports provide compelling evidence that type 2 diabetes impairs arteriogenesis and angiogenesis (4–10). Several observations from the current study, however, suggest this may not be the sole mechanism. First, limb perfusion

compared with MCAT mice (n = 24/group). *L*: Representative H&E stains of the control and ischemic limbs of WT and MCAT mice. *M*: Quantification of the ischemic lesion area (consisting of anucleate necrotic myofibers) was significantly larger in WT mice compared with MCAT mice (n = 6/group). *N*: The percentage of fibers with centralized nuclei was lower in WT compared with MCAT mice (n = 6 /group). *O*: Force-frequency relationships in isolated EDL muscles from control and ischemic limbs in WT and MCAT mice (n = 8/group). *P*: Peak specific force was significantly lower in the ischemic limb of WT mice, whereas MCAT mice showed a complete rescue in peak force in the ischemic EDL muscle. Data are mean ± SEM and were compared with two-way ANOVA followed by Tukey posttest or two-tailed Student t test. Nonparametric data (necrosis scores) were compared with Mann-Whitney test. HHB, deoxygenated hemoglobin/myoglobin; O_2HB, oxygenated hemoglobin/myglobin; SO_2, tissue saturation. Scale bars: 200 μm. *P < 0.05, **P < 0.01, [a]P < 0.05 for genotype effect, [b]P < 0.05 for ischemia effect. AUC, area under the curve; wks, weeks.

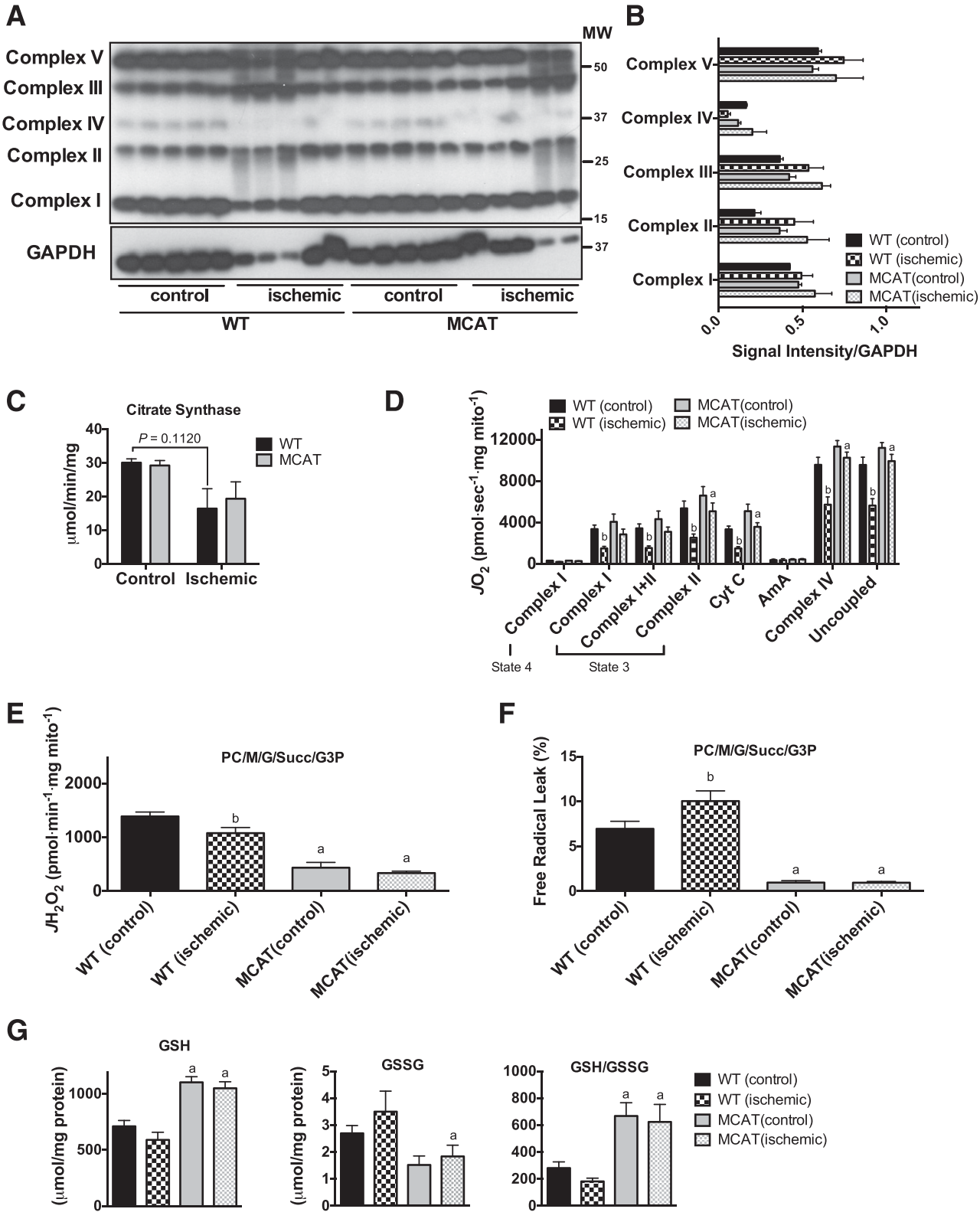

Figure 7—MCAT rescues mitochondrial respiratory function, decreases H_2O_2 emission, and maintains the cellular redox state in ischemic limb muscle. *A*: Western blotting for mitochondrial ETS proteins on control and ischemic limb EDL muscle from WT and MCAT mice (n = 5/group). *B*: Densitometry of Western blotting shows no genotype or ischemia effects on the abundance of proteins in the ETS. *C*: Citrate synthase activity was also not different between WT and MCAT mice (n = 5/group). *D*: High-resolution respirometry experiments performed on isolated skeletal muscle mitochondria show that the respiratory capacity was significantly lower in WT ischemic limbs compared with WT control limb muscle mitochondria (n = 8/group), which was rescued in the ischemic limb mitochondria from MCAT mice. *E*: Mitochondrial H_2O_2 emission under state 4 conditions with 25 μmol palmitoyl carnitine, 10 mmol glutamate, 2 mmol malate, 10 mmol succinate, and 10 mmol glycerol-3-phosphate was substantially lower in both control and ischemic limbs of MCAT mice,

measured by LDPI was reduced to a similar degree in HFD mice at both 6 and 16 weeks (~15% lower compared with LFD), but exacerbation of the ischemic myopathy was only evident in chronic HFD mice. Second, targeted measurements of paw tissue oxygenation and IF imaging for vessel density were not different between diets in either control or ischemic limbs. Third, mitochondrial catalase overexpression rescued the ischemic myopathy and limb necrosis in the absence of substantial improvements in limb blood flow or tissue oxygenation. Finally, catalase overexpression was robust in skeletal muscle, with only a slight increase in the vasculature of MCAT mice, which is presumably attributed to striated smooth muscle cells. Collectively, these observations provide strong evidence that the effects of HFD on ischemic myopathy cannot be entirely explained by impaired neovascularization in the ischemic limb. Our results clearly reveal a role for limb muscle mitochondria in this process, regardless of the respective dominant roles vascular or skeletal muscle cells play. It is likely that vascular and muscle insults collectively accumulate and affect each other until the outcomes reach a critical tipping point to cause outward pathological manifestations of the disease and/or functional consequences.

CLI is a devastating manifestation of PAD that carries significant risks for major amputation and death. Clinically, treatment options for CLI are limited to endovascular and revascularization surgical approaches with suboptimal long-term success rates. For these reasons, there is a dire need for novel therapeutic targets that may prevent/improve current treatment paradigms. In the current study, targeted overexpression of a key oxidant-scavenging enzyme (catalase) to the mitochondria protected against the ischemic myopathy enabled by chronic HFD. Importantly, rescue of ischemic myopathy in MCAT mice occurred despite clear evidence of a diabetic phenotype (i.e., obesity, glucose intolerance, and reduce insulin sensitivity) and no overt improvements in blood flow, tissue oxygenation, or vessel density. Interestingly, under chow-fed conditions in which the oxidant burden is low, MCAT did not improve recovery from HLI. In conjunction with the finding of lower mitochondrial H_2O_2-emitting potential in the ischemic limb, this observation suggests that ischemia-induced oxidative stress is not a major factor in limb pathology (16). However, the improvement in limb pathology in HFD-fed MCAT mice indicates that mitochondrial targeted therapies for PAD/CLI treatment may be most effective in high-risk patients in whom PAD/CLI occurs in the presence of other significant risk factors (i.e., diabetic or sedentary lifestyle) or genetic mitochondrial stressors (52).

It is important to acknowledge the unique pathophysiology of human PAD, in which patients often present clinically with reduced vascular density, impaired endothelial function, reduced skeletal muscle mitochondrial function, and decreased exercise performance/capacity. The potential negative effects of corresponding risk factors on the ability of each of the limb cellular compartments to survive and respond to chronic ischemia presents a complex paradigm when modeling clinical PAD in the preclinical setting. This is particularly pertinent when considering the complex relationship between skeletal muscle mitochondria and capillaries/endothelial cells (53,54), which may have functional implications for patients who manifest as intermittent claudicants with lower muscle capillary density. The experiments described in this study allow for the analysis of the effects of dietary overnutrition on the cells of the lower limb during the acute onset of ischemia in mice and suggest that corresponding muscle and vascular cell responses contribute to the overt disease phenotype. Distinct phenotypic manifestations of human PAD are thought to be akin to the response of different inbred mouse strains to limb ischemia (25–27). In fact, we recently found that BALB/c mice (akin to patients with CLI) exhibit significant myopathy and mitochondrial dysfunction in response to subacute limb ischemia (ameroid constrictors) despite similar vascular density, limb perfusion, and tissue oxygenation to C57BL6J mice (akin to claudicating/asymptomatic patients) (26,55). This clearly indicates the complexities of human PAD/CLI and indicates that a key to advancing therapeutic options for PAD/CLI is an increased understanding of the individual and coordinated cellular responses to ischemia.

In summary, the current study demonstrates that chronic high-fat feeding exacerbates ischemic myopathy following HLI. The specific combinations of diet, ischemia, and mice allowed us to uncover the influence that mitochondrial respiration and free radical leak have on the

consistent with increased scavenging by catalase overexpression (n = 8/group). *F*: Free radical leak (%), calculated by normalizing data from *E* by state 4 JO_2 measured in parallel experiments under identical substrate conditions, was also lower in the control and ischemic limbs of MCAT mice compared with WT mice (n = 8/group). *G*: GSH was significantly higher in the control and ischemic limb muscle of MCAT mice compared with that of WT mice; GSSG, oxidized form, was lower in both control and ischemic limbs of MCAT mice compared with those of WT mice, although statistical significance was only achieved in the ischemic limb; and the GSH/GSSG ratio was substantially higher in MCAT control and ischemic muscle compared with WT muscle, but no effect of ischemia was detected in either group (n = 5/group). Data are mean ± SEM and were compared with two-way ANOVA followed by Tukey posttest or two-tailed Student t test. $^aP < 0.05$ for genotype effect, $^bP < 0.05$ for ischemia effect. AmA, antimycin A; Complex $I_{(state\ 3)}$, glutamate + malate + adenosine diphosphate; Complex $I_{(state\ 4)}$, glutamate + malate; Complex $I+II_{(state\ 3)}$, glutamate + malate + adenosine diphosphate + succinate; Complex $II_{(state\ 3)}$, glutamate + malate + adenosine diphosphate + succinate + rotenone; Complex IV, ascorbate + N,N,N',N'-tetramethyl-p-phenylenediamine; Cyt c, cytochrome c; G, glutamate; G3P, glycerol-3-phosphate; M, malate; MW, molecular weight; PC, palmitoyl carnitine; Succ, succinate; Uncoupled, carbonyl cyanide-4-(trifluoromethoxy)phenylhydrazone.

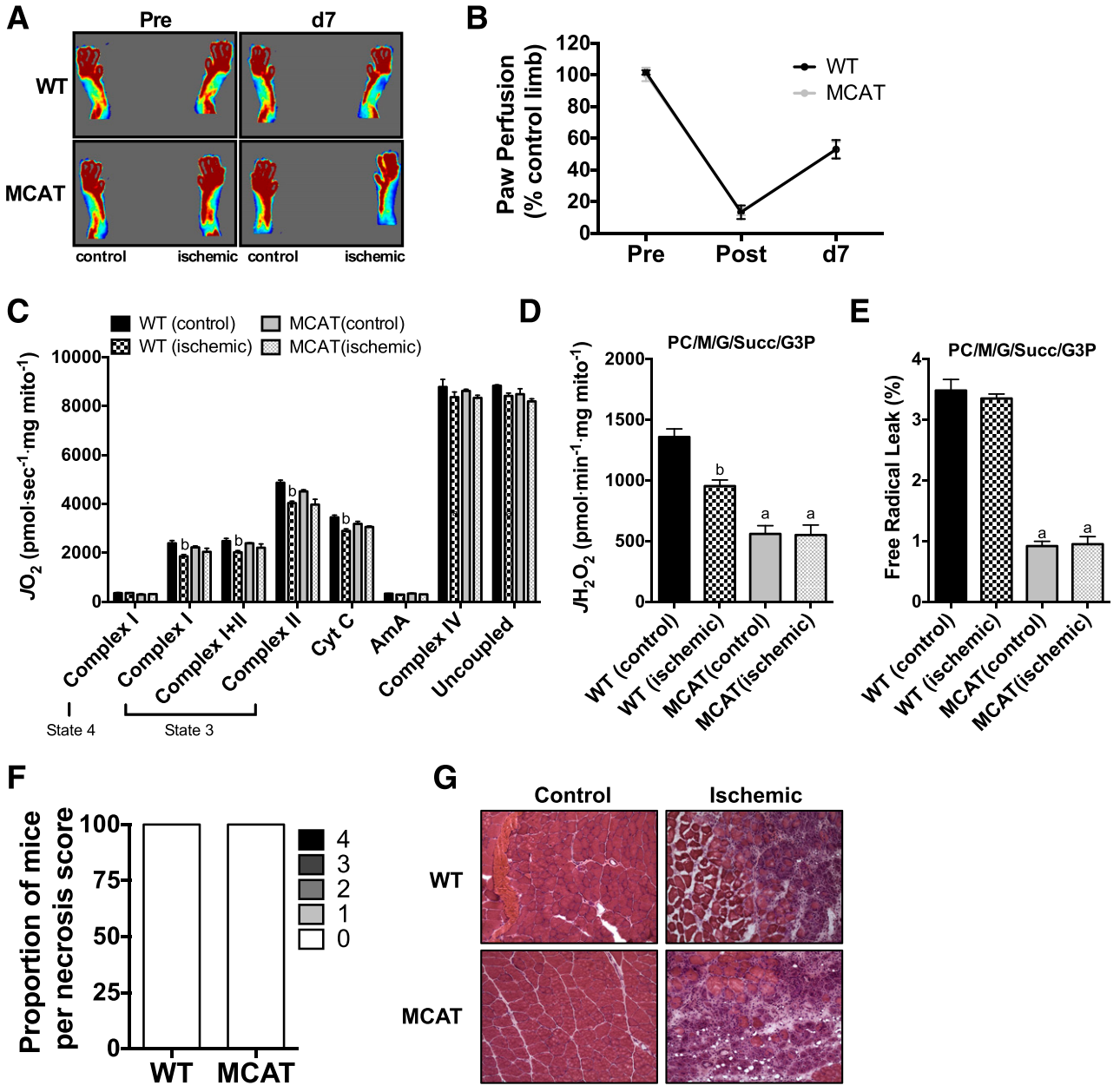

Figure 8—MCAT does not improve recovery from hindlimb ischemia in chow-fed mice. *A*: Representative LDPI images pre-HLI and 7 days post-HLI (d7). *B*: Quantification of LDPI flux demonstrates that paw perfusion recovery was not different between WT mice (n = 4) and MCAT mice (n = 4) on chow diet. *C*: High-resolution respirometry experiments performed on isolated skeletal muscle mitochondria show that the respiratory capacity was not different between WT and MCAT mice (n = 4/group) and ischemia induced a small, nonsignificant decrease in respiration. *D*: Mitochondrial H_2O_2 emission under state 4 conditions with 25 μmol palmitoyl carnitine, 10 mmol glutamate, 2 mmol malate, 10 mmol succinate, and 10 mmol glycerol-3-phosphate was substantially lower in both control and ischemic limbs of MCAT mice, consistent with increased scavenging by catalase overexpression (n = 4/group). *E*: Free radical leak (%), calculated by normalizing data from *D* by state 4 JO_2 measured in parallel experiments under identical substrate conditions, was also lower in the control and ischemic limbs of MCAT mice compared with those of WT mice (n = 4/group), but no ischemia effects were detected in either genotype. *F*: Proportions of necrosis scores at HLI day 7 for WT and MCAT mice on chow diet (n = 4/group). *G*: Representative H&E stains of the control and ischemic limbs of WT and MCAT mice fed a chow diet. Images were acquired at 20× magnification. Data are mean ± SEM and were compared with two-way ANOVA followed by Tukey posttest or two-tailed Student t test. Nonparametric data (necrosis scores) were compared with Mann-Whitney test. $^aP < 0.05$ for genotype effect, $^bP < 0.05$ for ischemia effect. AmA, antimycin A; Complex $I_{(state\ 3)}$, glutamate + malate + adenosine diphosphate; Complex $I_{(state\ 4)}$, glutamate + malate; Complex $I+II_{(state\ 3)}$, glutamate + malate + adenosine diphosphate + succinate; Complex $II_{(state\ 3)}$, glutamate + malate + adenosine diphosphate + succinate + rotenone; Complex IV, ascorbate + N,N,N',N'-tetramethyl-p-phenylenediamine; Cyt c, cytochrome c; G, glutamate; G3P, glycerol-3-phosphate; M, malate; PC, palmitoyl carnitine; Succ, succinate; Uncoupled, carbonyl cyanide-4-(trifluoromethoxy)phenylhydrazone.

manifestation of disease severity in the peripheral limb. These findings clinically parallel the idea that type 2 diabetes and overnutrition is sufficient to override the inherent protection provided by an individual's genetic predisposition toward mild PAD symptomology and, instead, result in tissue loss associated with CLI. In this instance, clinical interventions with mitochondrial antioxidant therapies may reduce morbidity outcomes. Altogether, these data highlight the link between ischemic mitochondria and limb muscle function and identify the mitochondria as a unique candidate for therapeutic intervention in situations in which multiple risk factors enable the most severe complications of PAD.

Funding. T.E.R. is supported by National Institutes of Health (NIH)/National Heart, Lung, and Blood Institute (NHLBI) grant F32-HL-129632. E.E.S. is supported by NIH/National Institute of Arthritis and Musculoskeletal and Skin Diseases grant R01-AR-066660. P.D.N. is supported by NIH/National Institute of Diabetes and Digestive and Kidney Diseases grant R01-DK-096907. J.M.M. is supported by NIH/NHLBI grants R00-HL-103797 and R01-HL-125695.

Duality of Interest. No potential conflicts of interest relevant to this article were reported.

Author Contributions. T.E.R. contributed to the design, researched data, and wrote the manuscript. C.A.S. and T.D.G. researched data and reviewed and edited the manuscript. E.E.S. reviewed and edited the manuscript and contributed to discussion. P.D.N. contributed to the design and reviewed and edited manuscript. J.M.M. contributed to the design, researched data, and wrote the manuscript. J.M.M. is the guarantor of this work and, as such, had full access to all the data in the study and takes responsibility for the integrity of the data and the accuracy of the data analysis.

References

1. Jude EB, Oyibo SO, Chalmers N, Boulton AJ. Peripheral arterial disease in diabetic and nondiabetic patients: a comparison of severity and outcome. Diabetes Care 2001;24:1433–1437

2. Beckman JA, Creager MA, Libby P. Diabetes and atherosclerosis: epidemiology, pathophysiology, and management. JAMA 2002;287:2570–2581

3. Malmstedt J, Leander K, Wahlberg E, Karlström L, Alfredsson L, Swedenborg J. Outcome after leg bypass surgery for critical limb ischemia is poor in patients with diabetes: a population-based cohort study. Diabetes Care 2008;31:887–892

4. Waltenberger J, Lange J, Kranz A. Vascular endothelial growth factor-A-induced chemotaxis of monocytes is attenuated in patients with diabetes mellitus: A potential predictor for the individual capacity to develop collaterals. Circulation 2000;102:185–190

5. Babu M, Durga Devi T, Mäkinen P, et al. Differential Promoter Methylation of Macrophage Genes Is Associated With Impaired Vascular Growth in Ischemic Muscles of Hyperlipidemic and Type 2 Diabetic Mice: Genome-Wide Promoter Methylation Study. Circ Res 2015;117:289–299

6. DiStasi MR, Mund JA, Bohlen HG, et al. Impaired compensation to femoral artery ligation in diet-induced obese mice is primarily mediated via suppression of collateral growth by Nox2 and p47phox. Am J Physiol Heart Circ Physiol 2015; 309:H1207–H1217

7. Moore SM, Zhang H, Maeda N, Doerschuk CM, Faber JE. Cardiovascular risk factors cause premature rarefaction of the collateral circulation and greater ischemic tissue injury. Angiogenesis 2015;18:265–281

8. Yan J, Tie G, Park B, Yan Y, Nowicki PT, Messina LM. Recovery from hind limb ischemia is less effective in type 2 than in type 1 diabetic mice: roles of endothelial nitric oxide synthase and endothelial progenitor cells. J Vasc Surg 2009;50:1412–1422

9. Hazarika S, Dokun AO, Li Y, Popel AS, Kontos CD, Annex BH. Impaired angiogenesis after hindlimb ischemia in type 2 diabetes mellitus: differential regulation of vascular endothelial growth factor receptor 1 and soluble vascular endothelial growth factor receptor 1. Circ Res 2007;101:948–956

10. Dunn LL, Simpson PJ, Prosser HC, et al. A critical role for thioredoxin-interacting protein in diabetes-related impairment of angiogenesis. Diabetes 2014;63:675–687

11. Park SW, Goodpaster BH, Strotmeyer ES, et al.; Health, Aging, and Body Composition Study. Accelerated loss of skeletal muscle strength in older adults with type 2 diabetes: the health, aging, and body composition study. Diabetes Care 2007;30:1507–1512

12. Leenders M, Verdijk LB, van der Hoeven L, et al. Patients with type 2 diabetes show a greater decline in muscle mass, muscle strength, and functional capacity with aging. J Am Med Dir Assoc 2013;14:585–592

13. Fisher-Wellman KH, Neufer PD. Linking mitochondrial bioenergetics to insulin resistance via redox biology. Trends Endocrinol Metab 2012;23:142–153

14. McDermott MM, Liu K, Tian L, et al. Calf muscle characteristics, strength measures, and mortality in peripheral arterial disease: a longitudinal study. J Am Coll Cardiol 2012;59:1159–1167

15. Cluff K, Miserlis D, Naganathan GK, et al. Morphometric analysis of gastrocnemius muscle biopsies from patients with peripheral arterial disease: objective grading of muscle degeneration. Am J Physiol Regul Integr Comp Physiol 2013;305:R291–R299

16. Weiss DJ, Casale GP, Koutakis P, et al. Oxidative damage and myofiber degeneration in the gastrocnemius of patients with peripheral arterial disease. J Transl Med 2013;11:230

17. Koutakis P, Weiss DJ, Miserlis D, et al. Oxidative damage in the gastrocnemius of patients with peripheral artery disease is myofiber type selective. Redox Biol 2014;2:921–928

18. Jain A, Liu K, Ferrucci L, et al. The Walking Impairment Questionnaire stair-climbing score predicts mortality in men and women with peripheral arterial disease. J Vasc Surg 2012;55:1662–1673.e1662

19. Thompson JR, Swanson SA, Haynatzki G, et al. Protein Concentration and Mitochondrial Content in the Gastrocnemius Predicts Mortality Rates in Patients With Peripheral Arterial Disease. Ann Surg 2015;261:605–610

20. Anderson EJ, Lustig ME, Boyle KE, et al. Mitochondrial H2O2 emission and cellular redox state link excess fat intake to insulin resistance in both rodents and humans. J Clin Invest 2009;119:573–581

21. Bonnard C, Durand A, Peyrol S, et al. Mitochondrial dysfunction results from oxidative stress in the skeletal muscle of diet-induced insulin-resistant mice. J Clin Invest 2008;118:789–800

22. Houstis N, Rosen ED, Lander ES. Reactive oxygen species have a causal role in multiple forms of insulin resistance. Nature 2006;440:944–948

23. Hoehn KL, Salmon AB, Hohnen-Behrens C, et al. Insulin resistance is a cellular antioxidant defense mechanism. Proc Natl Acad Sci USA 2009;106: 17787–17792

24. Chouchani ET, Pell VR, Gaude E, et al. Ischaemic accumulation of succinate controls reperfusion injury through mitochondrial ROS. Nature 2014;515: 431–435

25. Dokun AO, Keum S, Hazarika S, et al. A quantitative trait locus (LSq-1) on mouse chromosome 7 is linked to the absence of tissue loss after surgical hindlimb ischemia. Circulation 2008;117:1207–1215

26. McClung JM, McCord TJ, Southerland K, et al. Subacute limb ischemia induces skeletal muscle injury in genetically susceptible mice independent of vascular density. J Vasc Surg. 5 August 2015 [Epub ahead of print]

27. McClung JM, McCord TJ, Keum S, et al. Skeletal muscle-specific genetic determinants contribute to the differential strain-dependent effects of hindlimb ischemia in mice. Am J Pathol 2012;180:2156–2169

28. Fisher-Wellman KH, Lin CT, Ryan TE, et al. Pyruvate dehydrogenase complex and nicotinamide nucleotide transhydrogenase constitute an energy-consuming redox circuit. Biochem J 2015;467:271–280

29. Spangenburg EE, Le Roith D, Ward CW, Bodine SC. A functional insulin-like growth factor receptor is not necessary for load-induced skeletal muscle hypertrophy. J Physiol 2008;586:283–291
30. Brooks SV, Faulkner JA. Contractile properties of skeletal muscles from young, adult and aged mice. J Physiol 1988;404:71–82
31. Giustarini D, Dalle-Donne I, Milzani A, Fanti P, Rossi R. Analysis of GSH and GSSG after derivatization with N-ethylmaleimide. Nat Protoc 2013;8:1660–1669
32. Kand'ár R, Záková P, Lotková H, Kucera O, Cervinková Z. Determination of reduced and oxidized glutathione in biological samples using liquid chromatography with fluorimetric detection. J Pharm Biomed Anal 2007;43:1382–1387
33. Schriner SE, Linford NJ, Martin GM, et al. Extension of murine life span by overexpression of catalase targeted to mitochondria. Science 2005;308:1909–1911
34. Lee HY, Choi CS, Birkenfeld AL, et al. Targeted expression of catalase to mitochondria prevents age-associated reductions in mitochondrial function and insulin resistance. Cell Metab 2010;12:668–674
35. Pipinos II, Judge AR, Zhu Z, et al. Mitochondrial defects and oxidative damage in patients with peripheral arterial disease. Free Radic Biol Med 2006; 41:262–269
36. Pipinos II, Swanson SA, Zhu Z, et al. Chronically ischemic mouse skeletal muscle exhibits myopathy in association with mitochondrial dysfunction and oxidative damage. Am J Physiol Regul Integr Comp Physiol 2008;295:R290–R296
37. Taylor SM, Cull DL, Kalbaugh CA, et al. Comparison of interventional outcomes according to preoperative indication: a single center analysis of 2,240 limb revascularizations. J Am Coll Surg 2009;208:770–778; discussion 778–780
38. Kelley DE, He J, Menshikova EV, Ritov VB. Dysfunction of mitochondria in human skeletal muscle in type 2 diabetes. Diabetes 2002;51:2944–2950
39. Mootha VK, Lindgren CM, Eriksson KF, et al. PGC-1alpha-responsive genes involved in oxidative phosphorylation are coordinately downregulated in human diabetes. Nat Genet 2003;34:267–273
40. Patti ME, Butte AJ, Crunkhorn S, et al. Coordinated reduction of genes of oxidative metabolism in humans with insulin resistance and diabetes: Potential role of PGC1 and NRF1. Proc Natl Acad Sci USA 2003;100:8466–8471
41. Quinlan CL, Perevoshchikova IV, Hey-Mogensen M, Orr AL, Brand MD. Sites of reactive oxygen species generation by mitochondria oxidizing different substrates. Redox Biol 2013;1:304–312
42. Fisher-Wellman KH, Gilliam LA, Lin CT, Cathey BL, Lark DS, Neufer PD. Mitochondrial glutathione depletion reveals a novel role for the pyruvate dehydrogenase complex as a key H2O2-emitting source under conditions of nutrient overload. Free Radic Biol Med 2013;65:1201–1208
43. Berglund ED, Lustig DG, Baheza RA, et al. Hepatic glucagon action is essential for exercise-induced reversal of mouse fatty liver. Diabetes 2011;60: 2720–2729
44. Satapati S, Sunny NE, Kucejova B, et al. Elevated TCA cycle function in the pathology of diet-induced hepatic insulin resistance and fatty liver. J Lipid Res 2012;53:1080–1092
45. Mantena SK, Vaughn DP, Andringa KK, et al. High fat diet induces dysregulation of hepatic oxygen gradients and mitochondrial function in vivo. Biochem J 2009;417:183–193
46. McDermott MM, Liu K, Ferrucci L, et al. Decline in functional performance predicts later increased mobility loss and mortality in peripheral arterial disease. J Am Coll Cardiol 2011;57:962–970
47. Jain A, Liu K, Ferrucci L, et al. Declining walking impairment questionnaire scores are associated with subsequent increased mortality in peripheral artery disease. J Am Coll Cardiol 2013;61:1820–1829
48. Leeper NJ, Myers J, Zhou M, et al. Exercise capacity is the strongest predictor of mortality in patients with peripheral arterial disease. J Vasc Surg 2013;57:728–733
49. Matsubara Y, Matsumoto T, Aoyagi Y, et al. Sarcopenia is a prognostic factor for overall survival in patients with critical limb ischemia. J Vasc Surg 2015;61:945–950
50. Fu X, Zhu M, Zhang S, Foretz M, Viollet B, Du M. Obesity Impairs Skeletal Muscle Regeneration Through Inhibition of AMPK. Diabetes 2016;65:188–200
51. Hu Z, Wang H, Lee IH, et al. PTEN inhibition improves muscle regeneration in mice fed a high-fat diet. Diabetes 2010;59:1312–1320
52. Brass EP, Wang H, Hiatt WR. Multiple skeletal muscle mitochondrial DNA deletions in patients with unilateral peripheral arterial disease. Vasc Med 2000;5: 225–230
53. Pecorella SR, Potter JV, Cherry AD, et al. The HO-1/CO system regulates mitochondrial-capillary density relationships in human skeletal muscle. Am J Physiol Lung Cell Mol Physiol 2015;309:L857–L871
54. Glancy B, Hsu LY, Dao L, et al. In vivo microscopy reveals extensive embedding of capillaries within the sarcolemma of skeletal muscle fibers. Microcirculation 2014;21:131–147
55. Schmidt CA, Ryan TE, Lin CT, et al. Diminished force production and mitochondrial respiratory deficits are strain-dependent myopathies of subacute limb ischemia. J Vasc Surg. In press